This is an open access article published under an ACS AuthorChoice License, which permits copying and redistribution of the article or any adaptations for non-commercial purposes.

Journal of Medicinal Chemistry

Article

Cite This: J. Med. Chem. 2018, 61, 2052−2061

pubs.acs.org/jmc

Reduction of Circulating Cancer Cells and Metastases in Breast-Cancer Models by a Potent EphA2-Agonistic Peptide−Drug Conjugate

Ahmed F. Salem,[†,¶] Si Wang,[‡,¶] Sandrine Billet,[§,¶] Jie-Fu Chen,[§] Parima Udompholkul,[†] Luca Gambini,[†] Carlo Baggio,[†] Hsian-Rong Tseng,[∥] Edwin M. Posadas,[§] Neil A. Bhowmick,[§,⊥] and Maurizio Pellecchia*[,†]

[†]Division of Biomedical Sciences, School of Medicine, University of California, Riverside, 900 University Avenue, Riverside, California 92521, United States

[‡]Sanford-Burnham-Prebys Medical Discovery Institute, 10901 North Torrey Pines Road, La Jolla, California 92037, United States

[§]Department of Medicine, Cedars-Sinai Medical Center, 8700 Beverly Boulevard, Los Angeles, California 90048, United States

[∥]Department of Molecular & Medical Pharmacology, University of California, Los Angeles, 570 Westwood Plaza, Los Angeles, California 90095, United States

[⊥]Department of Research, Greater Los Angeles Veterans Administration, Los Angeles, California 90073, United States

Supporting Information

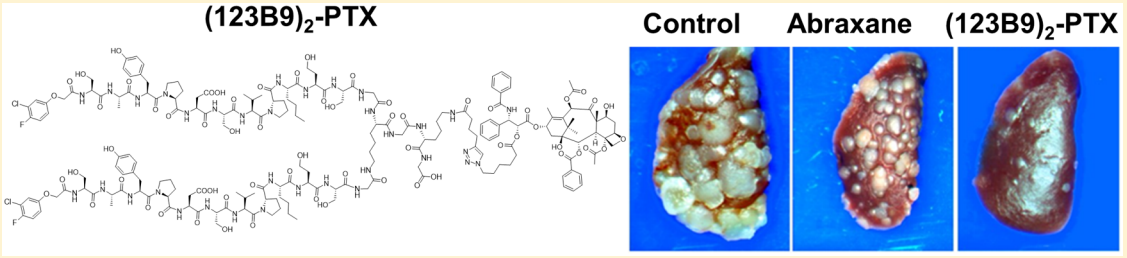

ABSTRACT: EphA2 overexpression has been associated with metastasis in multiple cancer types, including melanomas and ovarian, prostate, lung, and breast cancers. We have recently proposed the development of peptide−drug conjugates (PDCs) using agonistic EphA2-targeting agents, such as the YSA peptide or its optimized version, 123B9. Although our studies indicated that YSA− and 123B9−drug conjugates can selectively deliver cytotoxic drugs to cancer cells in vivo, the relatively low cellular agonistic activities (i.e., the high micromolar concentrations required) of the agents toward the EphA2 receptor remained a limiting factor to the further development of these PDCs in the clinic. Here, we report that a dimeric version of 123B9 can induce receptor activation at nanomolar concentrations. Furthermore, we demonstrated that the conjugation of dimeric 123B9 with paclitaxel is very effective at targeting circulating tumor cells and inhibiting lung metastasis in breast-cancer models. These studies represent an important step toward the development of effective EphA2-targeting PDCs.

INTRODUCTION

Tumor-specific cell-surface receptors represent potentially very attractive targets for the development of targeted deliveries of chemotherapies.[1,2] These receptors would allow in principle the design of agents that could selectively target malignant cells while sparing normal cells.[3,4] One such tumor-specific target is the EphA2 receptor.[5−11] Indeed, a high level of EphA2 has been detected in most solid tumors, including breast,[11] prostate,[12,13] pancreatic,[14−16] urinary bladder,[17] brain,[18−20] ovarian,[21] esophageal,[22] lung,[23] and stomach[24] cancers and melanomas,[25,26] and potentially also in certain types of leukemia.[27−30] During cancer progression, overexpression of the receptor EphA2 can lead to its ligand-independent pro-oncogenic activation, which is induced by reduced engagement with the ligand, ephrin-A. These pro-oncogenic effects of the unligated EphA2 receptor can be reversed by ligand stimulation, which triggers the intrinsic tumor-suppressive signaling pathways of EphA2, including the inhibition of the PI3K/Akt and ERK pathways,[31] Further interests in EphA2 signaling stem from the distinction between its physiological roles in tissue homeostasis, angiogenesis, and fetal development and its pathological role, which is associated with the metastasis of multiple cancer types, including breast cancer.[32−34] These observations argue for the development of small-molecule EphA2 agonists as potential tumor-intervention agents. Because the receptor's activation causes its internalization, antibody−drug conjugates (ADCs)[35] targeting the EphA2 ligand-binding domain (LBD) have been recently investigated. In particular, a recent Phase I study intended to evaluate increasing doses of

Received: December 15, 2017
Published: February 22, 2018

 © 2018 American Chemical Society

DOI: 10.1021/acs.jmedchem.7b01837
J. Med. Chem. 2018, 61, 2052−2061

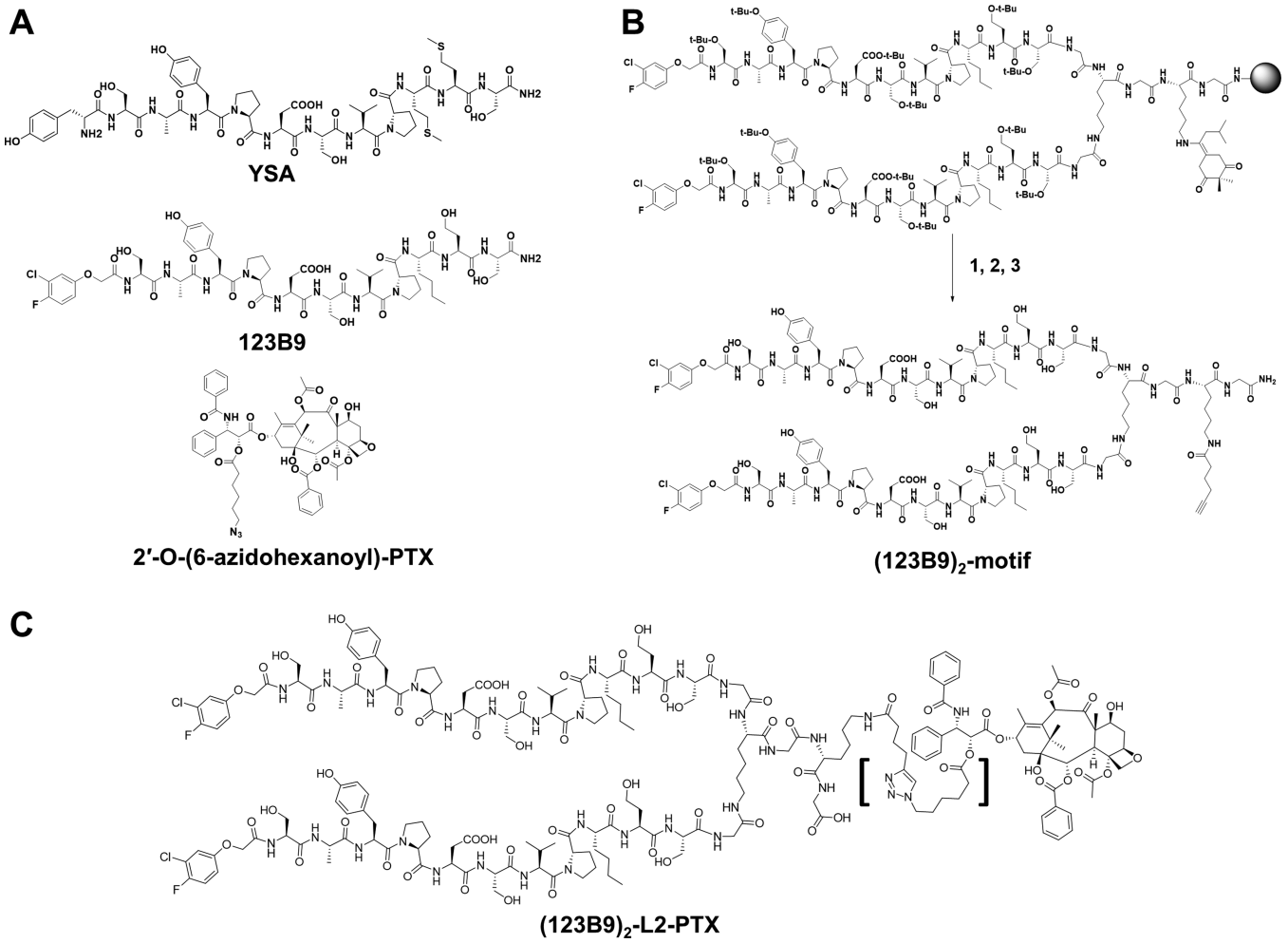

Figure 1. Chemical structures and general scheme for the synthesis of the reported agents. (A) Chemical structures of the YSA peptide, 123B9, and of the derivatized paclitaxel used for the conjugation. (B) General scheme for the synthesis of the $(123B9)_2$-motif. Regents and conditions: (1) NH_2NH_2, DMF, room temperature (rt), 30 min; (2) 5-hexynoic acid, HTBU, HOBt, DIEPA, DMF, rt, 12 h; (3) TFA, phenol, TIPS, water, rt, 3 h. (C) Chemical structure of $(123B9)_2$−L2−PTX. The L2 linker is highlighted by squared parentheses.

MEDI-547, an ADC composed of a human anti-EphA2 monoclonal antibody (1C1) linked to a cytotoxic auristatin derivative (maleimido-caproylmonomethyl auristatin phenylalanine, mcMMAF) was carried out in a small cohort of patients with solid tumors that had relapsed or were refractory to standard therapies.[36] However, the study was terminated because of the drug-related adverse effects noted at the starting dose. This could have been caused by cross-reactions between MEDI-547 and other proteins or insufficient subcellular internalization of the ADC.[36] Toxicity remains problematic because of EphA2's nonspecific distribution; therefore, EphA2 remains a high-priority target in need of a therapeutic agent. To address this need, we pursued a peptide-based targeting of taxanes. In particular, we sought to derive peptide−drug conjugates (PDCs) that could be used to increase taxane delivery to metastatic tumors. We elected to focus on PDCs that target the ephrin-binding pocket in the extracellular N-terminal domain of EphA2 using previously reported agonistic peptides.[26] The amino acid sequence YSAYPDSVPMMS (YSA), identified using a phage-display technique, has been shown to bind to the extracellular domain of EphA2 and promote receptor activation and internalization in several cancer-cell types.[37,38] We developed and further optimized an innovative antitriazole linker for the synthesis of EphA2-targeting peptide−drug conjugates to avoid the compatibility problems of disulfide and hydrazone linkers typical of ADCs.[39−42] This strategy of deriving YSA-based drug conjugates has been used to target prostate cancer, renal cancer, melanoma, and pancreatic cancer.[39−43] These previous studies identified agent 123B9 as a more plasma-stable compound, compared with YSA. Here, we report that a dimeric version of 123B9 can induce receptor activation at nanomolar concentrations, likely through the oligomerization of EphA2. Moreover, we showed that targeting EphA2 with a conjugation of the dimeric 123B9 with paclitaxel reduced circulating tumor cells and significantly inhibited lung metastasis in breast-cancer models.

RESULTS

Synthesis and Characterization of a 123B9-Based Dimeric PDC Targeting EphA2. The synthesis of dimeric 123B9 conjugated to paclitaxel, $(123B9)_2$−L2−PTX, followed the general schemes illustrated in Figure 1A. Dimeric 123B9 was generated by a solid-phase synthetic scheme that introduced a Lys-Gly-Lys-Gly moiety and orthogonal protecting groups, which allowed the synthesis of two 123B9 agents on the backbone and side chain of the first Lys; the second Lys side chain was used for the subsequent coupling with 5-

DOI: 10.1021/acs.jmedchem.7b01837
J. Med. Chem. 2018, 61, 2052−2061

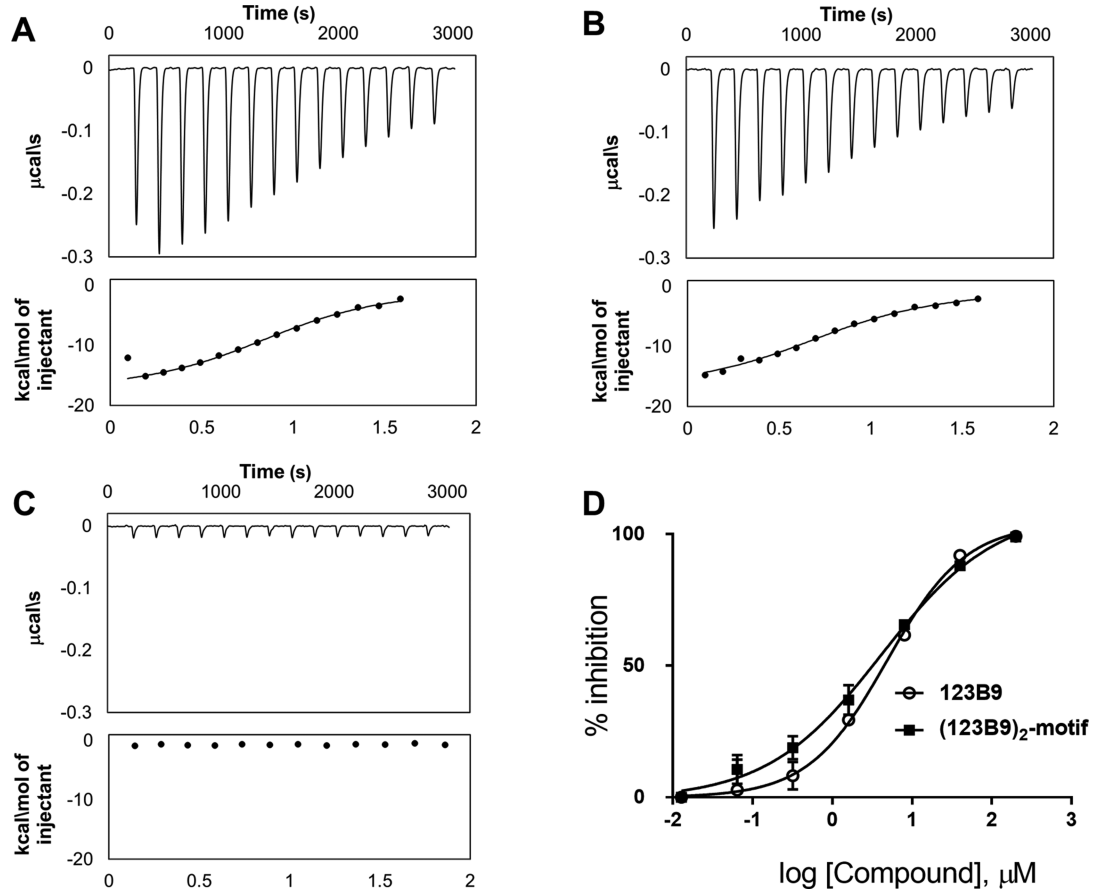

Figure 2. Biophysical- and biochemical-activity comparisons of 123B9 and the $(123B9)_2$-motif. (A) Isothermal-titration-calorimetry data relative to 123B9 (30 μM) titrated against EphA2-LBD (200 μM), resulting in a dissociation constant of 3.9 μM. (B) Isothermal-titration-calorimetry data relative to the $(123B9)_2$-motif against EphA2-LBD, resulting in a dissociation constant of 4.9 μM. (C) Isothermal-titration-calorimetry data relative to the $(123B9)_2$-motif against EphA4-LBD, showing no significant binding to this closely related ligand-binding domain. (D) Dose–response DELFIA curves for the displacement of biotinylated 123B9 from EphA2-LBD by compounds 123B9 and the $(123B9)_2$-motif (IC_{50} values of 4.9 and 4.1 μM, respectively).

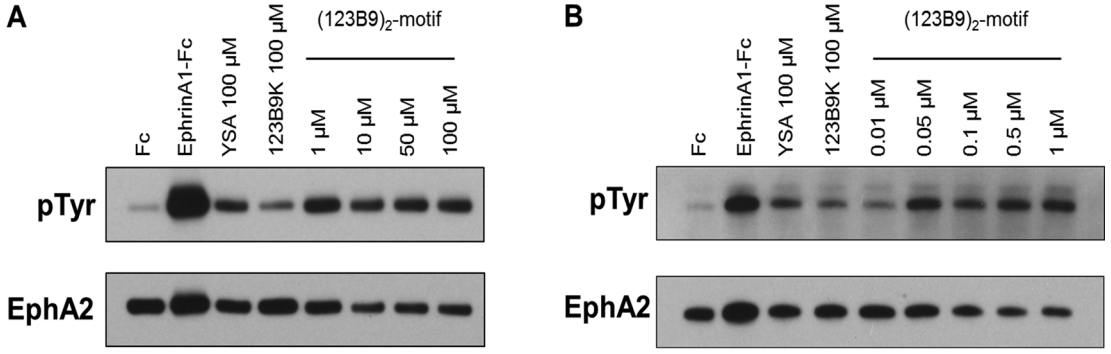

Figure 3. EphA2 ligand dimers potently stimulate the EphA2 receptor in submicromolar concentrations. EphA2-overexpressing HEK293*T*/17 cells were starved and then treated with clustered Fc, clustered ephrin-A1 Fc, YSA, 123B9, or the 123B9 dimers for 30 min. The cells were lysed, and then the EphA2 receptor was immunoprecipitated. The samples were blotted with an antiphosphotyrosine antibodies, and then stripped and reblotted with anti-EphA2 antibodies to ensure equal loading. The 123B9 dimers phosphorylated the tyrosine residues in the EphA2 receptors with 2000-fold lower concentrations than YSA or the 123B9 monomer.

hexynoic acid. To elongate the linker between the two 123B9 moieties, an additional Gly residue was added at the C-terminus of 123B9 (Figure 1B). The peptide–drug conjugate was subsequently generated by coupling the $(123B9)_2$-motif to an azido-hexanoyl paclitaxel group. Briefly, 2′-(6-azidohexanoyl)-*O*-paclitaxel and the $(123B9)_2$-motif in DMSO/water (4:1) were added to a solution of $CuSO_4$ (1.0 M) and sodium ascorbate (1.0 M) and continually stirred for 2 days. The product was purified on a reverse-phase C-18 column by HPLC with a gradient of 10–90% water/acetonitrile to give the desired agent (Figure 1C) as a white powder.

To further verify the binding affinity and selectivity of the resulting conjugates for the EphA2 ligand-binding domain (LBD), we expressed and purified the EphA2 and EphA4

DOI: 10.1021/acs.jmedchem.7b01837
J. Med. Chem. 2018, 61, 2052–2061

ligand-binding domains (EphA2-LBD and EphA4-LBD). These proteins were dissolved to final concentrations of 100 μM in 50 mM phosphate buffer (pH = 6.5) containing 100 mM NaCl. The isothermal-titration-calorimetry (ITC) measurements under these experimental conditions revealed that 123B9 and the $(123B9)_2$-motif bound to EphA2 with similar K_d values of 3.9 and 4.9 μM, respectively (Figure 2A,B). These similar values were expected for the agents when tested against the isolated ligand-binding domain, given that this domain did not present an appreciable dimerization propensity in solution. In contrast, much like 123B9, the $(123B9)_2$-motif had no appreciable binding to EphA4-LBD (Figure 2C). To further quantify the relative ability of the dimeric agent to displace EphA2-LBD−123B9 binding, we developed a dissociation-enhanced-lanthanide-fluorescent-immunoassay (DELFIA) platform using 96-well streptavidin-coated plates (PerkinElmer) and biotinylated 123B9. Both 123B9 and the $(123B9)_2$-motif were able to displace 123B9-biotin with comparable IC_{50} values of 4.9 and 4.1 μM, respectively, in agreement with the binding of the agents to monomeric EphA2-LBD (Figure 2D).

EphA2-Receptor Activation by Dimeric 123B9. Agonistic peptides have been previously shown to promote EphA2 phosphorylation (indicative of activation) in various cancer-cell lines at concentrations between 50 and 100 μM, which is 1 order of magnitude higher than the affinities of the peptides to the receptor in vitro (Figure 2). To assess $(123B9)_2$-mediated receptor activation, HEK293T cells stably transfected with EphA2 were tested. For the controls, ephrin-A1 Fc was used as a positive control, and Fc alone was used as a negative control. After treatment with test agents, immunoprecipitated EphA2 was probed with antiphosphotyrosine antibodies (P-Tyr) and reprobed with anti-EphA2 antibodies (Figure 3). As previously reported, YSA and 123B9 induced receptor activation at relatively high micromolar concentrations (Figure 3A), whereas the $(123B9)_2$-motif showed activation at all of the concentrations tested down to 1 μM. Subsequent testing of lower concentrations remarkably demonstrated that 10 nM concentrations of the $(123B9)_2$-motif induced receptor activation similar to that of ephrin-A1 Fc (Figure 3B).

Effect of $(123B9)_2$−L2−PTX on Circulating Tumor Cells in an Orthotopic Breast-Cancer-Metastasis Model. The antimetastatic capacities of $(123B9)_2$−L2−PTX were explored by examining its effects on circulating tumor cells (CTCs). The NanoVelcro system is a novel nanotechnology platform for rare-cell isolation used by our group. Its performance characteristics show a greater CTC-capture sensitivity for human prostate-cancer patients when compared with conventional CTC-capture methodologies, such as the CellSearch assay.[44,45] To assess the ability of $(123B9)_2$−L2−PTX to limit CTCs in vivo, we introduced triple-negative human MDA-MB-231 breast-cancer cells into the mammary fat pads of NOD SCID mice. The mice were monitored for the development of the primary tumors, which reached sizes of approximately 1 mm^3. At that point, the mice were treated intravenously with Abraxane or $(123B9)_2$−L2−PTX three times a week for a period of 2 weeks. The $(123B9)_2$−L2−PTX doses were 24.5 mg/kg, the molecular equivalent to the PTX doses (5 mg/kg) in the Abraxane group. We were able to distinguish the cancer cells from the immune cells in the circulation using immunofluorescent staining for pan-cytokeratin and CD45, respectively. We revealed reduced lymph-node involvement and reductions in regrowth at the sites of the primary tumors, corresponding with significantly reduced CTC in the $(123B9)_2$−L2−PTX-treatment group compared with in the Abraxane-treatment group (Figure 4A). Differential staining

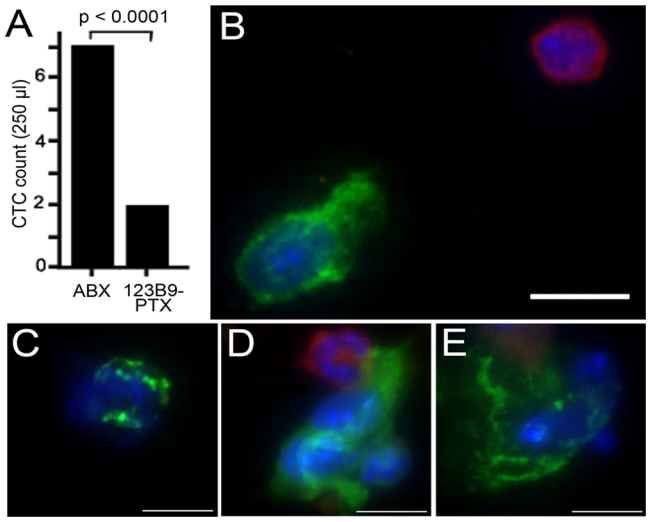

Figure 4. CTC evaluation using an orthotopic breast-cancer mouse metastatic model. CTC enumeration studies were done using NanoVelcro CTC Chips. (A) CTC counts in MDA-MB-231 breast-cancer cells orthotopically grafted into NOD-SCID mice treated with $(123B9)_2$−L2−PTX or Abraxane (ABX). The CTC counts in the $(123B9)_2$−L2−PTX group were significantly lower. (B) Captured cells directly stained for pan-cytokeratin (green) and CD45 (red) expression. (C) Pan-cytokeratin-expressing cells histologically evaluated as cancer. The cell clusters captured were elevated in the Abraxane-treated mice (D) compared with those from the $(123B9)_2$−L2−PTX-treated mice (E). In panels B−E, the scale bars represent 10 μm.

of the CTC for pan-cytokeratin and CD45 further demonstrated that $(123B9)_2$−L2−PTX reduced cancer-cell clusters (Figure 4B−E), especially strong indicators of metastasis.[46,47]

Effect of $(123B9)_2$−L2−PTX in Vivo on a Syngeneic Breast-Cancer-Metastasis Model. To assess the antimetastatic properties in a direct and quantitative manner, we used a triple-negative breast-cancer cell line, 4T1, a model derived from a spontaneous mammary-gland carcinoma from a BALB/c mouse. These cells, introduced to the animals through intracardiac injections, are known to metastasize to the lungs, lymph nodes, adrenal glands, ovaries, and bones. Fifteen days after the injections, the animals were treated with $(123B9)_2$−L2−PTX three times a week for a period of 2 weeks at a dose of 24.5 mg/kg, the equivalent to the PTX dose (5 mg/kg) in Abraxane group. The mice in the $(123B9)_2$−L2−PTX-treated group seemed to tolerate the therapy well, with negligible weight loss. We observed the clear and significant ($p < 0.0001$) beneficial effects of the dimer drug on lung metastasis (Figure 5A,B), with a reduction of the gross lung-metastasis count by more than 75% compared with those in the control and Abraxane groups. H&E staining revealed additional reductions of microscopic lung nodules in the $(123B9)_2$−L2−PTX group, compared with those in the Abraxane and control groups. Finally, examination of the metastatic tumors in each of the groups demonstrated a pronounced reduction in CD31-expressing vasculature by the $(123B9)_2$−L2−PTX group compared with those in the Abraxane and vehicle groups (Figure 5C). Hence, the dimerization of the EphA2-targeting

DOI: 10.1021/acs.jmedchem.7b01837
J. Med. Chem. 2018, 61, 2052−2061

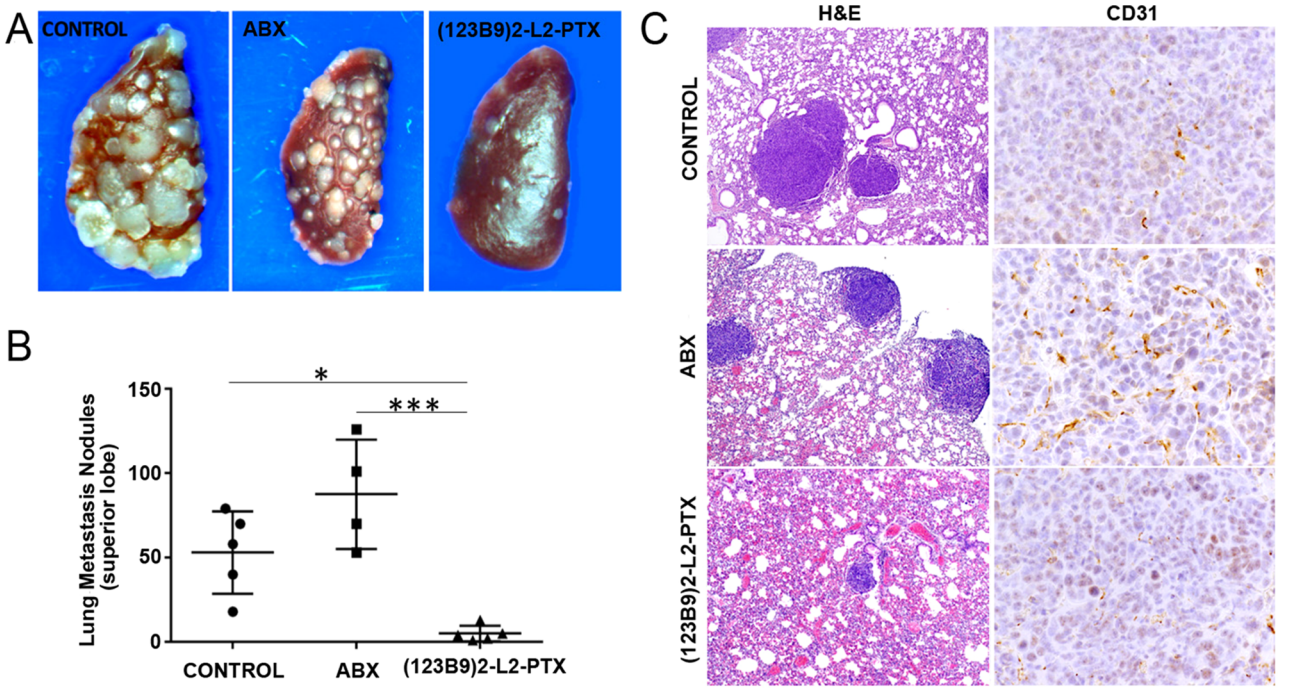

Figure 5. Syngeneic breast-cancer metastasis model. 4T1 cells were introduced to BALB/c mice by intracardiac injections and treated with $(123B9)_2$–L2–PTX or Abraxane. (A) Gross lung metastasis observed in the control, Abraxane, and $(123B9)_2$–L2–PTX groups. (B) Metastasis to the left lung superior lobe quantitated under the microscope (*$P < 0.05$, ***$P < 0.001$). (C) Histochemistry on lung sections from the three groups demonstrating the tumors (H&E at 4× magnification) and the vascularization by CD31 immuno-localization (40× magnification).

peptide improved the antimetastatic potential of the taxane over its albumin conjugation.

■ DISCUSSION AND CONCLUSIONS

The design of potent and selective agonistic peptides or small molecules that target the Eph-receptor ligand-binding domain has remained challenging. A variety of approaches have been proposed over the past decade, including high-throughput screening[48] and computational-docking strategies,[31,49−51] phage-display screening,[38] and NMR-based screening.[52−54] Each strategy accomplished the identification of potentially interesting compounds, but few have been fully validated in vivo. Although research is ongoing in the identification of potential small-molecule compounds,[31,49] most of the success has revolved around the discovery and optimizations of EphA2/ephrin antagonists,[48,50,51,55,56] although agonistic peptides remain the most studied EphA2-targeting agents in vivo.[6] Small agonistic peptides, however, are still only moderately potent and suffer from rapid degradation in plasma and clearance in vivo. Our previous studies with the EphA2-targeting YSA peptide (Figure 1A) and YSA-drug conjugates revealed that the rapid degradation of the agents in plasma was likely due to aminopeptidases, which caused rapid cleavage of the essential first amino acids.[41] On the basis of these observations, we designed an optimized YSA agent, namely, 123B9 (Figure 1B), in which the first Tyr residue was replaced by a bioisostere lacking the amino-terminus, conferring a long half-life to the agent in plasma and in vivo.[41,42] Further in vivo pharmacology and efficacy studies with the 123B9-drug conjugates also resulted in the optimization of the linker between the targeting peptides and the cytotoxic agents.[42] These data are consistent with our previous studies with unconjugated peptides and related paclitaxel conjugates.[39−41,57] Nonetheless, the abilities of these agents to cause receptor activation and internalization occur at relatively high concentrations of the agents (>50−100 μM),[38−40,58] likely limiting their potential translation to the clinic as effective targeted-delivery agents for tumor imaging or for capturing and killing circulating tumor cells. An interesting feature of EphA2 ligands is that their agonistic activities could be enhanced by properly clustering the targeting agent in nanoparticles or functionalized antibodies or by synthesizing dimers spaced by the appropriate linker.[58] For example, the ephrin ligands in isolation are not very effective in activating the receptor; they require clustering on Fc antibodies.[59] Indeed, it is known that only membrane-bound or Fc-clustered ephrin ligands can activate the receptor in vitro, and although soluble monomeric ligands can bind to the receptor, they only induce limited receptor autophosphorylation and activation.[59] Similarly, it was recently reported that EphA2-targeting agonistic peptides, when synthesized as dimeric molecules, displayed increased receptor activation in cell assays.[58] Using the YSA-analogue agonistic peptide, SWL (sequence SWLAYPGAVSYR), a dimeric agent made of two agents linked at the C-terminus by a six-carbon linker resulted in about a 13-fold increase in receptor-activation potency as compared with that of SWL, with significant receptor activation at 5−10 μM.[58] However, not surprisingly and similar to what we reported for YSA, the SWL dimer peptide presented a very short half-life in mouse serum, limiting its use in vivo.[58] Hence, we sought to first derive a dimeric version of our long-lived EphA2-agonistic agent 123B9 and assess its ability to retain the binding and selectivity for EphA2 in vitro and activate the receptor in cells. On the basis of the SWL-C6-dimer and the anticipated use of our dimeric agent for drug conjugation using our established antitriazole-linker click chemistry,[39−42] we designed and synthesized the $(123B9)_2$-motif as reported in Figure 1. This agent represents a dimeric version of 123B9, in which the linker between the molecules is equivalent in length

DOI: 10.1021/acs.jmedchem.7b01837
J. Med. Chem. 2018, 61, 2052−2061

to what was reported for the SWL-dimeric peptides but also presents the necessary alkyne for the subsequent drug conjugation (Figure 1). In vitro isothermal-titration-calorimetry (ITC) assays and displacement biochemical assays with purified EphA2-LBD confirmed that the dimeric agents bind to monomeric LBDs with a micromolar affinity that is surprisingly not similar to that of the monomeric agents, given that the isolated ligand-binding domains do not dimerize appreciably. In addition, no binding to the related EphA4 was observed under the same experimental conditions, again confirming the selectivity of these agents for EphA2 (Figure 2). When tested in cells for receptor activation, the $(123B9)_2$-motif was able to induce receptor phosphorylation at 1 μM, which was similar to what was produced by 100 μM YSA or 123B9 (Figure 3A). Moreover, when tested at lower concentrations, the $(123B9)_2$-motif revealed remarkable receptor activation in the nanomolar range, similar to what was accomplished by the Fc−ephrin ligand (Figure 3B). Hence, the dimeric $(123B9)_2$-motif represented to our knowledge the most potent synthetic EphA2-agonistic agent reported to date.

EphA2 expression is associated with increased metastatic behaviors in cancer cells. In our previous studies, we used a lung colonization and metastasis model of B16-F10-luc-G5 mouse melanoma cells with a 123B9−L2−PTX conjugate and compared the activity of the conjugate with that of albumin-bound paclitaxel (Abraxane).[42] As expected in that experiment, there were extensive tumor infiltrations into the lungs and other sites after 14 days of treatment. Both of the agents were equally effective in inhibiting lung colonization. However, Abraxane was not effective in preventing metastases to other organs, similar to the untreated control, whereas the 123B9−L2−PTX-treated mice displayed significantly reduced metastases.[42] Hence, we hypothesized that a more potent EphA2-targeting agent linked to a chemotherapeutic might be even more effective in targeting CTC and preventing migration to distant metastatic sites. For this purpose, we further synthesized $(123B9)_2$−L2−PTX, coupling the $(123B9)_2$-motif and 2′-(6-azidohexanoyl)-*O*-paclitaxel (Figure 1A). To test the ability of $(123B9)_2$−L2−PTX to selectively capture and kill circulating cancer cells in vivo, we employed a novel microfluidic-based capture approach, the NanoVelcro CTC chip. Circulating-tumor-cell capture has been used as a surrogate for determining the metastatic potentials of solid tumors. As such, CTC measurements can in principle provide new and important markers to monitor and predict the ability of a treatment to limit and prevent metastases.

Hence, when PTX was tested side by side with Abraxane at equimolar equivalents in an orthotopic model of triple-negative human MDA-MB-231 breast cancer, the CTC count was significantly reduced in the $(123B9)_2$−L2−PTX group compared with that in the group treated with Abraxane ($p < 0.0001$, Figure 4). As expected from these data, $(123B9)_2$−L2−PTX performed remarkably better than Abraxane in preventing lung metastases, with a reduction of the gross lung-metastasis count by more than 75% compared with that of Abraxane in an intracardiac breast-cancer metastasis model (Figure 5). This observation is in agreement with our previous study of 123B9−L2−PTX and Abraxane in a melanoma mouse model,[42] although the observed effect here is remarkably more impressive than what we had previously reported with 123B9−PTX.[42] Moreover, by virtue of the $(123B9)_2$−L2 moiety more effectively carrying the taxane than albumin, $(123B9)_2$−L2−PTX was capable of reducing the metastasis number and size by (1) targeting the primary tumor cells, (2) the diminishing CTCs, and (3) causing a marked reduction in tumor vasculature (CD31 staining, Figure 5), compared with Abraxane.

Paclitaxel remains to date one of the most effective broad-spectrum anticancer agents and is indeed approved for the treatment of a variety of cancers, including ovarian, breast, and lung cancers. However, given its low solubility in aqueous media, its requirement of long infusions and polyoxyethylated castor oil formulations, and the systemic distribution of the drug causing severe dose-limiting side effects, alternative PTX formulations have been proposed over the years.[60−62] Albumin-bound paclitaxel (Abraxane) presents several advantages over paclitaxel because of its aqueous solubility and the increased tumor uptake of the drug,[63] and it has received FDA approval thus far for metastatic breast cancer, advanced nonsmall-cell lung cancer, and more recently, metastatic pancreatic cancer. However, Abraxane shares the same side effects as paclitaxel, including dose-limiting bone-marrow suppression. We demonstrated recently that PDCs targeting EphA2-expressing cancer cells can deliver the cytotoxic drug to the tumor and the tumor vasculature, resulting in increased efficacy and reduced systemic toxicity.[39−43] A limitation of our previous EphA2-targeting PDCs resided in the targeting agents (YSA or 123B9), which caused receptor activation only at relatively high concentrations. The data reported here with the $(123B9)_2$-motif and $(123B9)_2$−L2−PTX clearly indicated that we have made a major step toward resolving this limitation. Currently, we envision further and more detailed pharmacology and toxicology studies and iterative structure−activity-relationship optimizations of $(123B9)_2$−L2−PTX to advance these discoveries into potentially a novel PDC for use in metastatic melanomas; breast, prostate, ovarian, and lung cancers; and potentially most solid tumors that depend on EphA2. Moreover, the $(123B9)_2$-motif or its further improved derivatives could be used not only to deliver cytotoxic agents but also to selectively introduce siRNA into cancer cells and to deliver imaging or other diagnostic agents.[64−67,42] For example, we have recently demonstrated that 123B9 conjugated with a near-infrared dye can be used to detect prostate cancer in mouse models.[43] Likewise, we anticipate that a conjugate of its dimeric version may have tremendous utility in devising more effective and sensitive cancer-imaging agents. Hence, we are confident that our present studies represent a novel and significant step that will open a wide range of opportunities for using more effective PDCs targeting EphA2 in the development of innovative diagnostics and cancer therapeutics targeting tumor metastases.

EXPERIMENTAL SECTION

Chemistry. *General.* All of the reagents and anhydrous solvents were obtained from commercial sources, including the Fmoc-protected amino acids and the resins for the solid-phase synthesis. Biologically active agents were purified to >95% purities, as determined by an HPLC Breeze from Waters Company using an Atlantis T3 5.0 μM 4.6 × 150 mm reverse-phase column. 1D and 2D NMR spectra were recorded on a Bruker 600 MHz instrument equipped with a TCI cryoprobe. The chemical shifts were reported in parts per million (δ) relative to ^{1}H (Me_4Si at 0.00 ppm), the coupling constants (J) were reported in Hz throughout, and the NMR-signal assignments were based on a variety of 1D and 2D experiments, including DEPT, 2D [^{13}C, ^{1}H]-HSQC, 2D [^{1}H, ^{1}H]-COSY, 2D [^{1}H, ^{1}H]-TOCSY, and 2D [^{1}H, ^{1}H]-HMBC experiments. Mass-spectrometry data were acquired on an Esquire LC00066 Mass Spectrometer, on an Agilent ESI-TOF

DOI: 10.1021/acs.jmedchem.7b01837
J. Med. Chem. 2018, 61, 2052−2061

Mass Spectrometer, or with a Bruker Daltonic Autoflex Maldi-Tof/Tof Mass Spectrometer.

Preparation of the (123B9)$_2$-Motif. The preparation of the (123B9)2-motif followed a solid-phase synthetic scheme similar to what we had previously adopted for the syntheses of the YSA-motif[39] and the 123B9-motif.[42] In the current protocol, 10.0 g of the fully protected peptide on a Rink amide resin was treated with 5% NH_2−NH_2 in DMF (3 × 40 mL, each 30 min) and was subsequently washed with DMF (3 × 50 mL) and THF (3 × 50 mL). This was followed by a treatment with 5-hexynoic acid (1.5 g, 13.38 mmol) in the presence of TBTU (6. 09 g, 16.05 mmol), HOBt (2.17 g, 16.05 mmol), and DIEPA (4.8 mL, 26.76 mmol) in DMF. For the lysine residue of the motif, we used an Fmoc-Lys(ivDde)-OH amino acid (*N*-α-Fmoc-*N*-ε-1-(4,4-dimethyl-2,6-dioxocyclohex-1-ylidene)-3-methylbutyl-L-lysine). This protection contained a sterically hindered Dde variant, rendering the ivDde protecting group considerably more stable. The mixture was filtered to remove the excess coupling agents after being shaken overnight, and the resin was washed with DMF (3 × 50 mL) and THF (3 × 50 mL) and dried under high vacuum. The coupling completion was monitored by the Kaiser ninhydrin test. The dried resin was further treated with TFA/phenol/TIPS/water (88:5:2:5, 30 mL) for 3 h, filtered, and washed with TFA (2 × 10 mL). The filtrate was concentrated under reduced pressure and transferred into centrifuge tubes, and then cold ether (50 mL) was added to these centrifuge tubes to produce the white precipitate. After the tubes were centrifuged for 10 min, the supernatant was decanted, and the precipitate was collected and purified by a reverse-phase C-18 column eluted with water/acetonitrile (0−30%) to provide the title compound (807 mg, yield 8.07%). ^{1}H NMR (600 MHz, DMSO-d_6): δ 8.16 (m, 7H), 7.50−8.10 (m, 20H), 7.42 (m, 3H), 7.06 (m, 5H), 6.97 (m, 3H), 4.52−4.53 (m, 5H), 4.38 (m, 3H), 4.20−4.35 (m, 15H), 4.14 (m, 1H), 4.00 (brs, 1H), 3.58−3.90 (m, 20H), 3.54 (m, 8H), 3.43 (m, 4H), 2.98 (m, 6H), 2.89 (m, 1H), 2.78 (m, 1H), 2.76 (s, 1H), 2.72 (m, 1H), 2.63 (m, 1H), 2.53 (m, 1H), 2.13−2.15 (m, 4H), 1.98 (m, 4H), 1.75−1.90 (m, 19H), 1.55−1.70 (m, 8H), 1.49 (m, 4H), 1.35 (m, 2H), 1.20−1.30 (m, 8H), 1.13 (d, J = 7.2 Hz, 6H), 0.88 (d, J = 7.2 Hz, 6H), 0.84 (brs, 12H). ^{13}C NMR (150 MHz, DMSO-d_6): δ 172.46, 172.31, 172.20, 172.09, 172.03, 171.96, 171.71, 171.35, 170.78, 170.71, 170.59, 170.08, 169.96, 169.67, 169.38, 169.24, 168.84, 167.59, 156.22, 154.75, 152.61 (J_{CF} = 245 Hz), 130.64, 128.11, 120.17, 120.04, 117.68, 117.54, 116.90, 115.65, 115.60, 115.36, 84.53, 71.88, 67.76, 62.17, 62.07, 60.13, 59.58, 57.96, 56.17, 55.58, 55.23, 54.83, 53.23, 52.99, 50.55, 50.45, 49.95, 49.02, 48.36, 47.51, 47.21, 42.57, 42.26, 38.89, 38.71, 36.19, 35.37, 35.30, 34.57, 32.24, 32.01, 31.77, 30.50, 29.37, 29.31, 29.23, 29.05, 27.62, 24.90, 24.83, 24.70, 23.08, 22.35, 21.47, 19.51, 18.69, 18.40, 18.26, 17.82, 14.27. MS (MALDI-TOF, m/z): $[M + Na]^+$ calcd for $C_{142}H_{204}Cl_2F_2N_{31}O_{47}$: 3226.37, found: 3226.41.

Preparation of (123B9)$_2$−L2−PTX. Solutions of $CuSO_4$ (1.0 M, 50 μL) and sodium ascorbate (1.0 M, 50 μL) were added to a stirred solution of 2′-(6-azidohexanoyl)-*O*-paclitaxel (103 mg, 0.103 mmol) and the 123B9-motif (422 mg, 0.103 mmol) in DMSO/water (4:1, 3.0 mL) and continually stirred for 2 days. ^{1}H NMR (600 MHz, DMSO-d_6): δ 7.50−8.16 (m, 46H), 6.68−7.50 (m, 19 H), 6.64 (d, J = 7.8 Hz, 4H), 6.29 (s, 1H), 5.81 (t, J = 9.0 Hz, 1H), 5.52 (t, J = 9.0 Hz, 1H), 5.41 (d, J = 9.0 Hz, 2H), 4.90 (d, J = 9.0 Hz, 1H), 4.54 (m, 4H), 4.41 (m, 2H), 4.20−4.38 (m, 19H), 4.17 (s, 2H), 4.11 (t, J = 7.2 Hz, 1H), 4.01 (m, 5H), 3.74 (m, 2H), 3.68 (m, 2H), 3.65 (s, 4H), 3.50−3.65 (m, 18H), 3.43 (m, 2H), 3.00 (m, 6H), 2.90 (m, 2H), 2.75 (m, 3H), 2.65 (m, 2H), 2.57 (t, J = 7.8 Hz, 2H), 2.31 (m, 1H), 2.22 (s, 3H), 2.09 (s, 3H), 2.08 (m, 3H), 1.98 (m, 4H), 1.80−1.90 (m, 16H), 1.78 (m, 3H), 1.76 (m, 2H), 1.65 (m, 6H), 1.49−1.55 (m, 6H), 1.49 (s, 3H), 1.37 (m, 1H), 1.19−1.30 (m, 13H), 1.15 (d, J = 7.2 Hz, 6H), 1.02 (s, 3H), 0.99 (s, 3H), 0.89 (d, J = 7.2 Hz, 6H), 0.83 (t, J = 7.2 Hz, 6H), 0.82 (s, 3H). ^{13}C NMR (150 MHz, DMSO-d_6): δ 202.78, 172.73, 172.31, 172.20, 172.03, 171.97, 171.36, 170.78, 170.59, 170.08, 169.96, 169.67, 169.39, 169.20, 168.84, 167.58, 166.77, 165.63, 158.83, 158.58, 156.44, 156.22, 154.75, 152.61 (J_{CF} = 245 Hz), 146.85, 144.36, 143.39, 141.15, 139.76, 137.70, 134.59, 133.94, 133.81, 131.96, 130.64, 130.35, 129.99, 129.13, 128.77, 128.65, 128.28, 128.11, 128.05, 127.81, 127.66, 127.46, 125.56, 125.37, 122.09, 120.68, 128.11, 128.05, 127.81, 127.66, 127.46, 125.56, 125.37, 122.09, 120.68, 120.53, 120.17, 120.04, 117.68, 117.53, 116.91, 115.64, 115.60, 115.36, 84.02, 80.66, 77.12, 75.69, 75.13, 74.90, 71.25, 70.81, 70.59, 67.76, 65.57, 62.17, 62.07, 60.13, 59.57, 57.96, 57.80, 56.17, 55.59, 55.23, 54.71, 54.40, 53.25, 52.99, 52.24, 51.86, 50.55, 50.45, 49.95, 49.31, 49.02, 48.57, 48.36, 47.51, 47.19, 46.49, 43.21, 42.36, 42.26, 38.89, 38.74, 36.93, 36.19, 36.10, 35.30, 34.80, 33.32, 32.01, 31.88, 31.79, 31.16, 30.53, 29.72, 29.37, 29.06, 27.77, 27.02, 26.73, 25.67, 25.60, 25.10, 24.90, 24.83, 24.19, 23.12, 22.98, 22.75, 22.35, 21.79, 21.09, 19.51, 18.69, 18.40, 14.27, 10.20. MS (MALDI-TOF, m/z): $[M + H]^+$ calcd for $C_{195}H_{264}Cl_2F_2N_{35}O_{62}$: 4195.79, found: 4196.91. The product was purified on a reverse-phase C-18 column by HPLC with a gradient of 10−90% water/acetonitrile to give the title compound (299 mg, 69%) as a white powder (95% purity).

Binding and Displacement Assays. EphA2-LBD and EphA4-LBD were expressed and purified as we previously reported.[42] Isothermal-titration-calorimetry (ITC) measurements were obtained with a TA Instruments microcalorimeter. For the in vivo studies, all of the drugs were diluted in 10% Tween-80, 10% DMSO, and 80% PBS. For the dissociation-enhanced lanthanide-fluorescent immunoassays (DELFIAs), 100 μL of a 1 μM biotin-123B9 solution was added to each well of 96-well streptavidin-coated plates (PerkinElmer) and incubated for 2 h. The plates were subsequently washed three times to remove the unbound biotin-123B9. After the washing steps, 25 μL solutions of 0.712 μM EphA2-LBD were preincubated with 2.5 μL of serial dilutions of the test compounds for 15 min, and 11 μL of each mixture was added to an 89 μL solution of 4.17 nM Eu−N1-labeled anti-6×His antibody (PerkinElmer) and incubated for 1 h. At the end of the incubation period, a second washing step was performed to remove the unbound protein−Eu antibody complexes that were displaced by the test compounds. Subsequently, 200 μL of the DELFIA enhancement solution (PerkinElmer) was added to each well, which was followed by a 10 min incubation. Fluorescence readings were then measured using the VICTOR X5 microplate reader (PerkinElmer) with excitation and emission wavelengths of 340 and 615 nm, respectively. All of the protein, peptide, and antibody solutions were prepared in a DELFIA assay buffer (PerkinElmer), and the incubations were performed at room temperature. The fluorescence readings were normalized to that of the DMSO control and reported as percent inhibition. The IC_{50} values were analyzed using GraphPad Prism Version 6.

Preparation of Viral Particles and Establishment of the EphA2-Expressing Cell Line. Human embryonic kidney (HEK) 293T/17 cells were purchased from ATCC and grown in Dulbecco's modified eagle medium (DMEM) with 10% fetal calf serum (FCS) at 37 °C and 5% CO_2. The cells were transfected with the EphA2 lentiviral plasmid (EX-A0125-Lv105) using the Lenti-Pac HIV Expression Packing Kit (GeneCopoeia, Inc.) to produce lentivirus particles according to manufacturer's protocol. After 2 days, viral particles were collected and filtered. Stable HEK 293T/17 cells overexpressing EphA2 were established by transducing fresh HEK 293T/17 cells with the viral particles and selecting the cells that overexpressed EphA2 with 1 μg/mL puromycin 2 days post-transduction. EphA2 overexpression was confirmed by a Western blot.

EphA2 Stimulation and Immunoprecipitation. The EphA2 stable cell line was plated in 6-well plates. The following day, the complete media was replaced with serum-free DMEM for 2 h, so that the cells were starved. The starved cells were stimulated with 0.5−1 μg/mL clustered mouse ephrin-A1 Fc or Fc (R&D systems) and with goat anti-human IgG Fc (Abcam, catalogue no. ab97221) for 30 min. During the stimulation, the indicated doses of YSA, 123B9, or the 123B9 dimers were added to each well. The control condition was treated with 1% DMSO. The stimulated cells were lysed with cell lysis buffer (20 mM Tris, pH 7.4, 120 mM NaCl, 1% Triton X-100, 0.5% sodium deoxycholate, 0.1% SDS, 1% IGEPAL, 5 mM EDTA) supplemented with EDTA-free Protease Inhibitor Cocktail and PhosStop (Sigma-Aldrich) for 30 min on ice. The cell lysates were then centrifuged for 10 min at 13 000 rpm and 4 °C to clear off the cell debris. Protein concentrations were quantified using a BCA Protein Assay kit (ThermoFisher), and the sample concentrations were

DOI: 10.1021/acs.jmedchem.7b01837
J. Med. Chem. 2018, 61, 2052−2061

adjusted to 1 μg/μL for all of the samples. The preclear steps for the cell lysates were performed using Pierce Protein A/G Agarose beads (ThermoFisher) for 1 h at 4 °C. The cell lysates and beads were centrifuged, and the supernatants were each incubated with 2 μg of mouse anti-EphA2-receptor antibodies (ThermoFisher, catalogue no. 1C11A12) at 4 °C overnight. The next day, the cell-lysate−antibody complexes were incubated with A/G agarose beads for 2 h at room temperature. After several washes, the target protein was eluted by being heated in 2× NuPAGE LDS sample buffer and NuPAGE antioxidant (ThermoFisher) for 5 min at 90 °C. The samples were loaded into 4−12% NuPAGE Bis-Tris precast gels and transferred to PVDF membranes. The membranes were blocked with 5% BSA in TBS and 0.1% Tween (TBST) for 1 h and then incubated with 1:3000 dilutions of mouse anti-phosphotyrosine antibodies (BD Biosciences, catalogue no. 610000, clone PY20) for 1 h. The antigen−antibody complexes were visualized using a Clarity Western ECL kit (BIO-RAD). The membranes were washed and stripped using the Restore Western Blot Stripping Buffer for 1 h and subsequently blocked with 5% nonfat milk in TBST. This was followed by a 1 h incubation with primary mouse anti-EphA2-receptor antibodies at 1:2000 dilutions. The membranes were then washed with TBST and incubated with goat anti-mouse HRP. The bands were visualized as mentioned previously.

In Vivo Allogeneic Breast-Cancer-Metastasis Model. Animal studies were carried out in accordance with the approved Cedars-Sinai Institutional Animal Care and Use Committee (IACUC) protocol. In order to evaluate $(123B9)_2$−L2−PTX on metastasis and more specifically on CTC, we used a basal MDA-MB-231 human breast carcinoma (1×10^6 cells) orthotopically injected into the mammary fat pads of NOD SCID mice. Once the primary tumors reached sizes of approximately 1 mm^3, the mice were intravenously treated with $(123B9)_2$−L2−PTX three times a week for a period of 2 weeks at a dose of 24.5 mg/kg, the molecular equivalent of the PTX dose (5 mg/kg) in the Abraxane group. When each animal was sacrificed, whole blood was collected, and CTC was estimated. $(123B9)_2$−PTX was dissolved in an aqueous formulation containing 84% PBS, 8% DMSO, and 8% Tween-20 and injected in a 100 μL final volume.

In Vivo Syngeneic Breast-Cancer-Metastasis Model. Mouse triple-negative 4T1 breast-cancer cells (1×10^5 cells) were injected into the left ventricles of hearts, which served as the syngeneic metastasis model. Fifteen days after injection, the animals were treated with $(123B9)_2$−L2−PTX or Abraxane three times a week for a period of 2 weeks at the previously indicated doses.

Immunohistochemical Analyses. CD31 staining was done by immunochemistry. Briefly, paraffin-embedded sections were deparaffinized in xylene, rehydrated through graded ethanol, and then submerged into citric acid buffer for the heat-induced antigenic retrieval. They were then blocked with 10% bovine serum albumin, incubated with the CD31 primary antibodies at 4 °C overnight, and developed using the DAKO ChemMate Envision Kit/HRP (Dako-Cytomation). They were then counterstained with hematoxylin, dehydrated, cleared, and mounted.

NanoVelcro Chip for Single CTC Isolation. NanoVelcro CTC assays represented a unique rare-cell sorting method that enabled the detection, isolation, and characterization of CTCs in peripheral blood. The NanoVelcro Chip was composed of (1) a cell-affinity substrate coated with poly(lactic-*co*-glycolic acid) (PLGA) nanofibers and (2) an overlaid PDMS chaotic mixer. This chip was used in conjunction with an LCM microscope to isolate the captured CTCs.[68] In brief, the PLGA-nanofibers covalently functionalized with streptavidin enabled the selective capture of CTCs labeled with biotinylated anti-EpCAM antibodies. This surface facilitated CTC capture through its unique topography. After the CTCs were immobilized on the substrate, the CTCs were stained with FITC-labeled anticytokeratin (for the epithelia) and TRITC-labeled anti-CD45 (for the immune cells). The CTCs were defined as cytokeratin-expressing cells that were absent of CD45 expression and whose morphology could be confirmed by a board-certified pathologist using bright-field microscopy.

■ ASSOCIATED CONTENT

Supporting Information

The Supporting Information is available free of charge on the ACS Publications website at DOI: 10.1021/acs.jmedchem.7b01837.

Biological data cited in Figures 2 and 3 (CSV)

■ AUTHOR INFORMATION

Corresponding Author

*E-mail: maurizio.pellecchia@ucr.edu. Tel.: (951) 827-7829.

ORCID

Hsian-Rong Tseng: 0000-0001-9028-8527

Maurizio Pellecchia: 0000-0001-5179-470X

Author Contributions

¶A.F.S., S.W., and S.B. contributed equally to this work

Notes

The authors declare no competing financial interest.

■ ACKNOWLEDGMENTS

Financial support was obtained in part by the NIH with NCI grants CA149668 and CA168517. M.P. holds the Daniel Hays Chair in Cancer Research at the School of Medicine at the University of California, Riverside (UCR). P.U. is a recipient of the 2017−2018 Pease Cancer Fellowship through the Division of Biomedical Sciences, School of Medicine, UCR.

■ ABBREVIATIONS USED

EphA2-LBD, ephrin type-A receptor 2 ligand-binding domain; PTX, paclitaxel; ABX, Abraxane; CTC, circulating tumor cells; PLGA, poly(lactic-*co*-glycolic acid)

■ REFERENCES

(1) Sugahara, K. N.; Teesalu, T.; Karmali, P. P.; Kotamraju, V. R.; Agemy, L.; Greenwald, D. R.; Ruoslahti, E. Coadministration of a tumor-penetrating peptide enhances the efficacy of cancer drugs. *Science* **2010**, *328*, 1031−1035.

(2) Teesalu, T.; Sugahara, K. N.; Ruoslahti, E. Tumor-penetrating peptides. *Front. Oncol.* **2013**, *3*, 216.

(3) Coffman, K. T.; Hu, M.; Carles-Kinch, K.; Tice, D.; Donacki, N.; Munyon, K.; Kifle, G.; Woods, R.; Langermann, S.; Kiener, P. A.; Kinch, M. S. Differential EphA2 epitope display on normal versus malignant cells. *Cancer Res.* **2003**, *63*, 7907−7912.

(4) Zelinski, D. P.; Zantek, N. D.; Stewart, J. C.; Irizarry, A. R.; Kinch, M. S. EphA2 overexpression causes tumorigenesis of mammary epithelial cells. *Cancer Res.* **2001**, *61*, 2301−2306.

(5) Ireton, R. C.; Chen, J. EphA2 receptor tyrosine kinase as a promising target for cancer therapeutics. *Curr. Cancer Drug Targets* **2005**, *5*, 149−157.

(6) Tandon, M.; Vemula, S. V.; Mittal, S. K. Emerging strategies for EphA2 receptor targeting for cancer therapeutics. *Expert Opin. Ther. Targets* **2011**, *15*, 31−51.

(7) Wykosky, J.; Debinski, W. The EphA2 receptor and ephrinA1 ligand in solid tumors: function and therapeutic targeting. *Mol. Cancer Res.* **2008**, *6*, 1795−1806.

(8) Pasquale, E. B. Eph receptors and ephrins in cancer: bidirectional signalling and beyond. *Nat. Rev. Cancer* **2010**, *10*, 165−180.

(9) Biao-Xue, R.; Xi-Guang, C.; Shuan-Ying, Y.; Wei, L.; Zong-Juan, M. EphA2-dependent molecular targeting therapy for malignant tumors. *Curr. Cancer Drug Targets* **2011**, *11*, 1082−1097.

(10) Beauchamp, A.; Debinski, W. Ephs and ephrins in cancer: ephrin-A1 signalling. *Semin. Cell Dev. Biol.* **2012**, *23*, 109−115.

(11) Ogawa, K.; Pasqualini, R.; Lindberg, R. A.; Kain, R.; Freeman, A. L.; Pasquale, E. B. The ephrin-A1 ligand and its receptor, EphA2, are

DOI: 10.1021/acs.jmedchem.7b01837
J. Med. Chem. 2018, 61, 2052−2061

expressed during tumor neovascularization. *Oncogene* **2000**, *19*, 6043−6052.
(12) Walker-Daniels, J.; Coffman, K.; Azimi, M.; Rhim, J. S.; Bostwick, D. G.; Snyder, P.; Kerns, B. J.; Waters, D. J.; Kinch, M. S. Overexpression of the EphA2 tyrosine kinase in prostate cancer. *Prostate* **1999**, *41*, 275−280.
(13) Zeng, G.; Hu, Z.; Kinch, M. S.; Pan, C. X.; Flockhart, D. A.; Kao, C.; Gardner, T. A.; Zhang, S.; Li, L.; Baldridge, L. A.; Koch, M. O.; Ulbright, T. M.; Eble, J. N.; Cheng, L. High-level expression of EphA2 receptor tyrosine kinase in prostatic intraepithelial neoplasia. *Am. J. Pathol.* **2003**, *163*, 2271−2276.
(14) Duxbury, M. S.; Ito, H.; Zinner, M. J.; Ashley, S. W.; Whang, E. E. Ligation of EphA2 by Ephrin A1-Fc inhibits pancreatic adenocarcinoma cellular invasiveness. *Biochem. Biophys. Res. Commun.* **2004**, *320*, 1096−1102.
(15) Duxbury, M. S.; Ito, H.; Zinner, M. J.; Ashley, S. W.; Whang, E. E. EphA2: a determinant of malignant cellular behavior and a potential therapeutic target in pancreatic adenocarcinoma. *Oncogene* **2004**, *23*, 1448−1456.
(16) Mudali, S. V.; Fu, B.; Lakkur, S. S.; Luo, M.; Embuscado, E. E.; Iacobuzio-Donahue, C. A. Patterns of EphA2 protein expression in primary and metastatic pancreatic carcinoma and correlation with genetic status. *Clin. Exp. Metastasis* **2007**, *23*, 357−365.
(17) Abraham, S.; Knapp, D. W.; Cheng, L.; Snyder, P. W.; Mittal, S. K.; Bangari, D. S.; Kinch, M.; Wu, L.; Dhariwal, J.; Mohammed, S. I. Expression of EphA2 and ephrin A-1 in carcinoma of the urinary bladder. *Clin. Cancer Res.* **2006**, *12*, 353−360.
(18) Wang, L. F.; Fokas, E.; Bieker, M.; Rose, F.; Rexin, P.; Zhu, Y.; Pagenstecher, A.; Engenhart-Cabillic, R.; An, H. X. Increased expression of EphA2 correlates with adverse outcome in primary and recurrent glioblastoma multiforme patients. *Oncol. Rep.* **2008**, *19*, 151−156.
(19) Wykosky, J.; Gibo, D. M.; Stanton, C.; Debinski, W. EphA2 as a novel molecular marker and target in glioblastoma multiforme. *Mol. Cancer Res.* **2005**, *3*, 541−551.
(20) Binda, E.; Visioli, A.; Giani, F.; Lamorte, G.; Copetti, M.; Pitter, K. L.; Huse, J. T.; Cajola, L.; Zanetti, N.; DiMeco, F.; De Filippis, L.; Mangiola, A.; Maira, G.; Anile, C.; De Bonis, P.; Reynolds, B. A.; Pasquale, E. B.; Vescovi, A. L. The EphA2 receptor drives self-renewal and tumorigenicity in stem-like tumor-propagating cells from human glioblastomas. *Cancer Cell* **2012**, *22*, 765−780.
(21) Merritt, W. M.; Thaker, P. H.; Landen, C. N., Jr.; Deavers, M. T.; Fletcher, M. S.; Lin, Y. G.; Han, L. Y.; Kamat, A. A.; Gershenson, D. M.; Kinch, M. S.; Sood, A. K. Analysis of EphA2 expression and mutant p53 in ovarian carcinoma. *Cancer Biol. Ther.* **2006**, *5*, 1357−1360.
(22) Miyazaki, T.; Kato, H.; Fukuchi, M.; Nakajima, M.; Kuwano, H. EphA2 overexpression correlates with poor prognosis in esophageal squamous cell carcinoma. *Int. J. Cancer* **2003**, *103*, 657−663.
(23) Faoro, L.; Singleton, P. A.; Cervantes, G. M.; Lennon, F. E.; Choong, N. W.; Kanteti, R.; Ferguson, B. D.; Husain, A. N.; Tretiakova, M. S.; Ramnath, N.; Vokes, E. E.; Salgia, R. EphA2 mutation in lung squamous cell carcinoma promotes increased cell survival, cell invasion, focal adhesions, and mammalian target of rapamycin activation. *J. Biol. Chem.* **2010**, *285*, 18575−18585.
(24) Yuan, W. J.; Ge, J.; Chen, Z. K.; Wu, S. B.; Shen, H.; Yang, P.; Hu, B.; Zhang, G. W.; Chen, Z. H. Over-expression of EphA2 and ephrinA-1 in human gastric adenocarcinoma and its prognostic value for postoperative patients. *Dig. Dis. Sci.* **2009**, *54*, 2410−2417.
(25) Hess, A. R.; Seftor, E. A.; Gardner, L. M.; Carles-Kinch, K.; Schneider, G. B.; Seftor, R. E.; Kinch, M. S.; Hendrix, M. J. Molecular regulation of tumor cell vasculogenic mimicry by tyrosine phosphorylation: role of epithelial cell kinase (Eck/EphA2). *Cancer Res.* **2001**, *61*, 3250−3255.
(26) Margaryan, N. V.; Strizzi, L.; Abbott, D. E.; Seftor, E. A.; Rao, M. S.; Hendrix, M. J.; Hess, A. R. EphA2 as a promoter of melanoma tumorigenicity. *Cancer Biol. Ther.* **2009**, *8*, 279−288.
(27) Takahashi, Y.; Itoh, M.; Nara, N.; Tohda, S. Effect of Eph-ephrin signaling on the growth of human leukemia cells. *Anticancer research* **2014**, *34*, 2913−2918.
(28) Trinidad, E. M.; Zapata, A. G.; Alonso-Colmenar, L. M. Eph-ephrin bidirectional signaling comes into the context of lymphocyte transendothelial migration. *Cell adhesion & migration* **2010**, *4*, 363−367.
(29) Alonso-C, L. M.; Trinidad, E. M.; de Garcillan, B.; Ballesteros, M.; Castellanos, M.; Cotillo, I.; Munoz, J. J.; Zapata, A. G. Expression profile of Eph receptors and ephrin ligands in healthy human B lymphocytes and chronic lymphocytic leukemia B-cells. *Leuk. Res.* **2009**, *33*, 395−406.
(30) Guan, M.; Liu, L.; Zhao, X.; Wu, Q.; Yu, B.; Shao, Y.; Yang, H.; Fu, X.; Wan, J.; Zhang, W. Copy number variations of EphA3 are associated with multiple types of hematologic malignancies. *Clinical lymphoma, myeloma & leukemia* **2011**, *11*, 50−53.
(31) Petty, A.; Myshkin, E.; Qin, H.; Guo, H.; Miao, H.; Tochtrop, G. P.; Hsieh, J. T.; Page, P.; Liu, L.; Lindner, D. J.; Acharya, C.; MacKerell, A. D., Jr.; Ficker, E.; Song, J.; Wang, B. A small molecule agonist of EphA2 receptor tyrosine kinase inhibits tumor cell migration in vitro and prostate cancer metastasis in vivo. *PLoS One* **2012**, *7*, e42120.
(32) Saito, T.; Masuda, N.; Miyazaki, T.; Kanoh, K.; Suzuki, H.; Shimura, T.; Asao, T.; Kuwano, H. Expression of EphA2 and E-cadherin in colorectal cancer: correlation with cancer metastasis. *Oncol. Rep.* **2004**, *11*, 605−611.
(33) Taddei, M. L.; Parri, M.; Angelucci, A.; Onnis, B.; Bianchini, F.; Giannoni, E.; Raugei, G.; Calorini, L.; Rucci, N.; Teti, A.; Bologna, M.; Chiarugi, P. Kinase-dependent and -independent roles of EphA2 in the regulation of prostate cancer invasion and metastasis. *Am. J. Pathol.* **2009**, *174*, 1492−1503.
(34) Fang, W. B.; Brantley-Sieders, D. M.; Parker, M. A.; Reith, A. D.; Chen, J. A kinase-dependent role for EphA2 receptor in promoting tumor growth and metastasis. *Oncogene* **2005**, *24*, 7859−7868.
(35) Jackson, D.; Gooya, J.; Mao, S.; Kinneer, K.; Xu, L.; Camara, M.; Fazenbaker, C.; Fleming, R.; Swamynathan, S.; Meyer, D.; Senter, P. D.; Gao, C.; Wu, H.; Kinch, M.; Coats, S.; Kiener, P. A.; Tice, D. A. A human antibody-drug conjugate targeting EphA2 inhibits tumor growth in vivo. *Cancer Res.* **2008**, *68*, 9367−9374.
(36) Annunziata, C. M.; Kohn, E. C.; LoRusso, P.; Houston, N. D.; Coleman, R. L.; Buzoianu, M.; Robbie, G.; Lechleider, R. Phase 1, open-label study of MEDI-547 in patients with relapsed or refractory solid tumors. *Invest. New Drugs* **2013**, *31*, 77−84.
(37) Koolpe, M.; Dail, M.; Pasquale, E. B. An ephrin mimetic peptide that selectively targets the EphA2 receptor. *J. Biol. Chem.* **2002**, *277*, 46974−46979.
(38) Mitra, S.; Duggineni, S.; Koolpe, M.; Zhu, X.; Huang, Z.; Pasquale, E. B. Structure-activity relationship analysis of peptides targeting the EphA2 receptor. *Biochemistry* **2010**, *49*, 6687−6695.
(39) Wang, S.; Placzek, W. J.; Stebbins, J. L.; Mitra, S.; Noberini, R.; Koolpe, M.; Zhang, Z.; Dahl, R.; Pasquale, E. B.; Pellecchia, M. Novel targeted system to deliver chemotherapeutic drugs to EphA2-expressing cancer cells. *J. Med. Chem.* **2012**, *55*, 2427−2436.
(40) Wang, S.; Noberini, R.; Stebbins, J. L.; Das, S.; Zhang, Z.; Wu, B.; Mitra, S.; Billet, S.; Fernandez, A.; Bhowmick, N. A.; Kitada, S.; Pasquale, E. B.; Fisher, P. B.; Pellecchia, M. Targeted delivery of paclitaxel to EphA2-expressing cancer cells. *Clin. Cancer Res.* **2013**, *19*, 128−137.
(41) Barile, E.; Wang, S.; Das, S. K.; Noberini, R.; Dahl, R.; Stebbins, J. L.; Pasquale, E. B.; Fisher, P. B.; Pellecchia, M. Design, synthesis and bioevaluation of an EphA2 receptor-based targeted delivery system. *ChemMedChem* **2014**, *9*, 1403−1412.
(42) Wu, B.; Wang, S.; De, S. K.; Barile, E.; Quinn, B. A.; Zharkikh, I.; Purves, A.; Stebbins, J. L.; Oshima, R. G.; Fisher, P. B.; Pellecchia, M. Design and characterization of novel EphA2 agonists for targeted delivery of chemotherapy to cancer Cells. *Chem. Biol.* **2015**, *22*, 876−887.
(43) Quinn, B. A.; Wang, S.; Barile, E.; Das, S. K.; Emdad, L.; Sarkar, D.; De, S. K.; Morvaridi, S. K.; Stebbins, J. L.; Pandol, S. J.; Fisher, P.

DOI: 10.1021/acs.jmedchem.7b01837
J. Med. Chem. 2018, 61, 2052−2061

B.; Pellecchia, M. Therapy of pancreatic cancer via an EphA2 receptor-targeted delivery of gemcitabine. *Oncotarget* **2016**, *7*, 17103−17110.
(44) Hou, S.; Chen, J. F.; Song, M.; Zhu, Y.; Jan, Y. J.; Chen, S. H.; Weng, T. H.; Ling, D. A.; Chen, S. F.; Ro, T.; Liang, A. J.; Lee, T.; Jin, H.; Li, M.; Liu, L.; Hsiao, Y. S.; Chen, P.; Yu, H. H.; Tsai, M. S.; Pisarska, M. D.; Chen, A.; Chen, L. C.; Tseng, H. R. Imprinted nanovelcro microchips for isolation and characterization of circulating fetal trophoblasts: toward non-invasive prenatal diagnostics. *ACS Nano* **2017**, *11*, 8167−8177.
(45) Chen, J. F.; Zhu, Y.; Lu, Y. T.; Hodara, E.; Hou, S.; Agopian, V. G.; Tomlinson, J. S.; Posadas, E. M.; Tseng, H. R. Clinical applications of nanovelcro rare-cell assays for detection and characterization of circulating tumor cells. *Theranostics* **2016**, *6*, 1425−1439.
(46) Sarioglu, A. F.; Aceto, N.; Kojic, N.; Donaldson, M. C.; Zeinali, M.; Hamza, B.; Engstrom, A.; Zhu, H.; Sundaresan, T. K.; Miyamoto, D. T.; Luo, X.; Bardia, A.; Wittner, B. S.; Ramaswamy, S.; Shioda, T.; Ting, D. T.; Stott, S. L.; Kapur, R.; Maheswaran, S.; Haber, D. A.; Toner, M. A microfluidic device for label-free, physical capture of circulating tumor cell clusters. *Nat. Methods* **2015**, *12*, 685−691.
(47) Au, S. H.; Storey, B. D.; Moore, J. C.; Tang, Q.; Chen, Y. L.; Javaid, S.; Sarioglu, A. F.; Sullivan, R.; Madden, M. W.; O'Keefe, R.; Haber, D. A.; Maheswaran, S.; Langenau, D. M.; Stott, S. L.; Toner, M. Clusters of circulating tumor cells traverse capillary-sized vessels. *Proc. Natl. Acad. Sci. U. S. A.* **2016**, *113*, 4947−4952.
(48) Giorgio, C.; Incerti, M.; Corrado, M.; Rusnati, M.; Chiodelli, P.; Russo, S.; Callegari, D.; Ferlenghi, F.; Ballabeni, V.; Barocelli, E.; Lodola, A.; Tognolini, M. Pharmacological evaluation of new bioavailable small molecules targeting Eph/ephrin interaction. *Biochem. Pharmacol.* **2018**, *147*, 21−29.
(49) Petty, A.; Idippily, N.; Bobba, V.; Geldenhuys, W. J.; Zhong, B.; Su, B.; Wang, B. Design and synthesis of small molecule agonists of EphA2 receptor. *Eur. J. Med. Chem.* **2018**, *143*, 1261−1276.
(50) Hassan-Mohamed, I.; Giorgio, C.; Incerti, M.; Russo, S.; Pala, D.; Pasquale, E. B.; Zanotti, I.; Vicini, P.; Barocelli, E.; Rivara, S.; Mor, M.; Lodola, A.; Tognolini, M. UniPR129 is a competitive small molecule Eph-ephrin antagonist blocking in vitro angiogenesis at low micromolar concentrations. *Br. J. Pharmacol.* **2014**, *171*, 5195−5208.
(51) Tognolini, M.; Incerti, M.; Pala, D.; Russo, S.; Castelli, R.; Hassan-Mohamed, I.; Giorgio, C.; Lodola, A. Target hopping as a useful tool for the identification of novel EphA2 protein-protein antagonists. *ChemMedChem* **2014**, *9*, 67−72.
(52) Wu, B.; De, S. K.; Kulinich, A.; Salem, A. F.; Koeppen, J.; Wang, R.; Barile, E.; Wang, S.; Zhang, D.; Ethell, I.; Pellecchia, M. Potent and selective EphA4 agonists for the treatment of ALS. *Cell Chem. Biol.* **2017**, *24*, 293−305.
(53) Wu, B.; Barile, E.; De, S. K.; Wei, J.; Purves, A.; Pellecchia, M. High-Throughput Screening by nuclear magnetic resonance (HTS by NMR) for the identification of PPIs antagonists. *Curr. Top. Med. Chem.* **2015**, *15*, 2032−2042.
(54) Wu, B.; Zhang, Z.; Noberini, R.; Barile, E.; Giulianotti, M.; Pinilla, C.; Houghten, R. A.; Pasquale, E. B.; Pellecchia, M. HTS by NMR of combinatorial libraries: a fragment-based approach to ligand discovery. *Chem. Biol.* **2013**, *20*, 19−33.
(55) Incerti, M.; Tognolini, M.; Russo, S.; Pala, D.; Giorgio, C.; Hassan-Mohamed, I.; Noberini, R.; Pasquale, E. B.; Vicini, P.; Piersanti, S.; Rivara, S.; Barocelli, E.; Mor, M.; Lodola, A. Amino acid conjugates of lithocholic acid as antagonists of the EphA2 receptor. *J. Med. Chem.* **2013**, *56*, 2936−2947.
(56) Castelli, R.; Tognolini, M.; Vacondio, F.; Incerti, M.; Pala, D.; Callegari, D.; Bertoni, S.; Giorgio, C.; Hassan-Mohamed, I.; Zanotti, I.; Bugatti, A.; Rusnati, M.; Festuccia, C.; Rivara, S.; Barocelli, E.; Mor, M.; Lodola, A. Delta(5)-cholenoyl-amino acids as selective and orally available antagonists of the Eph-ephrin system. *Eur. J. Med. Chem.* **2015**, *103*, 312−324.
(57) Wu, B.; Wang, S.; De, S. K.; Barile, E.; Quinn, B. A.; Zharkikh, I.; Purves, A.; Stebbins, J. L.; Oshima, R. G.; Fisher, P. B.; Pellecchia, M. Design and characterization of novel EphA2 agonists for targeted delivery of chemotherapy to cancer cells. *Chem. Biol.* **2015**, *22*, 876−887.
(58) Duggineni, S.; Mitra, S.; Lamberto, I.; Han, X.; Xu, Y.; An, J.; Pasquale, E. B.; Huang, Z. Design and synthesis of potent bivalent peptide agonists targeting the EphA2 receptor. *ACS Med. Chem. Lett.* **2013**, *4*, 344−348.
(59) Davis, S.; Gale, N. W.; Aldrich, T. H.; Maisonpierre, P. C.; Lhotak, V.; Pawson, T.; Goldfarb, M.; Yancopoulos, G. D. Ligands for eph-related receptor tyrosine kinases that require membrane attachment or clustering for activity. *Science* **1994**, *266*, 816−819.
(60) Bakrania, A. K.; Variya, B. C.; Patel, S. S. Novel targets for paclitaxel nano formulations: hopes and hypes in triple negative breast cancer. *Pharmacol. Res.* **2016**, *111*, 577−591.
(61) Nehate, C.; Jain, S.; Saneja, A.; Khare, V.; Alam, N.; Dubey, R. D.; Gupta, P. N. Paclitaxel formulations: challenges and novel delivery options. *Curr. Drug Delivery* **2014**, *11*, 666−686.
(62) Singla, A. K.; Garg, A.; Aggarwal, D. Paclitaxel and its formulations. *Int. J. Pharm.* **2002**, *235*, 179−192.
(63) Chen, N.; Brachmann, C.; Liu, X.; Pierce, D. W.; Dey, J.; Kerwin, W. S.; Li, Y.; Zhou, S.; Hou, S.; Carleton, M.; Klinghoffer, R. A.; Palmisano, M.; Chopra, R. Albumin-bound nanoparticle (nab) paclitaxel exhibits enhanced paclitaxel tissue distribution and tumor penetration. *Cancer Chemother. Pharmacol.* **2015**, *76*, 699−712.
(64) Patel, A. R.; Chougule, M.; Singh, M. EphA2 targeting pegylated nanocarrier drug delivery system for treatment of lung cancer. *Pharm. Res.* **2014**, *31*, 2796−2809.
(65) Xie, X.; Yang, Y.; Lin, W.; Liu, H.; Liu, H.; Yang, Y.; Chen, Y.; Fu, X.; Deng, J. Cell-penetrating peptide-siRNA conjugate loaded YSA-modified nanobubbles for ultrasound triggered siRNA delivery. *Colloids Surf., B* **2015**, *136*, 641−650.
(66) Cai, W.; Ebrahimnejad, A.; Chen, K.; Cao, Q.; Li, Z. B.; Tice, D. A.; Chen, X. Quantitative radioimmuno PET imaging of EphA2 in tumor-bearing mice. *Eur. J. Nucl. Med. Mol. Imaging* **2007**, *34*, 2024−2036.
(67) Liu, Y.; Lan, X.; Wu, T.; Lang, J.; Jin, X.; Sun, X.; Wen, Q.; An, R. (99m)Tc-labeled SWL specific peptide for targeting EphA2 receptor. *Nucl. Med. Biol.* **2014**, *41*, 450−456.
(68) Jiang, R.; Lu, Y. T.; Ho, H.; Li, B.; Chen, J. F.; Lin, M.; Li, F.; Wu, K.; Wu, H.; Lichterman, J.; Wan, H.; Lu, C. L.; OuYang, W.; Ni, M.; Wang, L.; Li, G.; Lee, T.; Zhang, X.; Yang, J.; Rettig, M.; Chung, L. W.; Yang, H.; Li, K. C.; Hou, Y.; Tseng, H. R.; Hou, S.; Xu, X.; Wang, J.; Posadas, E. M. A comparison of isolated circulating tumor cells and tissue biopsies using whole-genome sequencing in prostate cancer. *Oncotarget* **2015**, *6*, 44781−44793.

DOI: 10.1021/acs.jmedchem.7b01837
J. Med. Chem. 2018, 61, 2052−2061